Available online at www.sciencedirect.com
SCIENCE DIRECT
Journal of Power Sources 156 (2006) 748–754
JOURNAL OF POWER SOURCES
www.elsevier.com/locate/jpowsour

Resistance distribution in electrochemical capacitors with spiral-wound structure

J.P. Zheng *, Z.N. Jiang

Department of Electrical and Computer Engineering, Florida A&M University and Florida State University, Tallahassee, FL 32310, USA

Received 10 April 2005; accepted 15 May 2005
Available online 3 August 2005

Abstract

The distribution of internal resistance in a Panasonic 10 F, 2.5 V electrochemical capacitor comprised of activated carbon electrode and organic electrolyte was analyzed. It was found that in the direction along the electrode surface, the resistance of the cell was mainly determined by the current collector and was $1.7 \times 10^{-3}\ \Omega\,cm^{-1}$. In the direction perpendicular to the electrode surface, the resistance was dependent on the applied pressure and a minimum resistance of $13.66\ \Omega\,cm^2$ was obtained at an applied pressure of about $1\ kg\,cm^{-2}$. The resistance distribution at the applied pressure of $1\ kg\,cm^{-2}$ was 0.86, 1.91 and $8.11\ \Omega\,cm^2$ contributing to the electrode carbon material, contact between the current collector and electrode and separator/electrolyte, respectively. A transmission line model was used to describe the cell resistance with dependence parameters, electrode length and the location of the electrical leads.

Keywords: Internal resistance; Electrochemical capacitors; Spiral-wound structure

1. Introduction

The maximum current density and power density of electrochemical (EC) capacitors are limited by the internal resistance, which are contributed by the electrical and ionic resistances. The ionic resistance depends on the ionic conductivity of the electrolyte, the porosity of the electrode and separator/membrane paper, the thickness of the electrode and membrane paper. During pulsed and transient performance, the amount of ions (from the electrolyte) near the electrode surface can also be a dominating factor [1–3]. The EC capacitors can be divided into two types according to their structural configuration. The first type is a bipolar structure, which is mainly used for making capacitors with a low capacitance value and high operational voltage. EC capacitors using aqueous electrolytes a often use this kind of structure. The internal resistance distribution in EC capacitors with a bipolar structure was investigated and reported in a previous paper [4]. The second type is a spiral-wound structure, which is used for single cell capacitors with capacitance ranging from mili-farads to thousands of farads. Most EC capacitors that use organic electrolytes often use this kind of structure. In this paper, we will provide a detailed analysis of the distribution of resistance inside a capacitor made of activated carbon electrode materials and organic electrolytes.

2. Capacitor structure

A Panasonic capacitor rated 10 F and 2.5 V was chosen for the internal resistance study. The capacitor was made with spiral-wound structure as shown in Fig. 1. Activated carbon powder (specific surface area about $2000\ m^2\,g^{-1}$) [5,6] was used as the electrode material and was coated on both surfaces of an aluminum foil (20 μm-thick), which was used as a current collector. The water-soluble material acted as a binding agent. The binder material is believed to the polysaccharides or cellulose groups [6]. A pair of electrodes was then wound interlaying a separator between them. A porous paper

* Corresponding author. Tel.: +1 850 410 6464; fax: +1 850 410 6479.
E-mail address: zheng@eng.fsu.edu (J.P. Zheng).

0378-7753/$ – see front matter © 2005 Published by Elsevier B.V.
doi:10.1016/j.jpowsour.2005.05.089

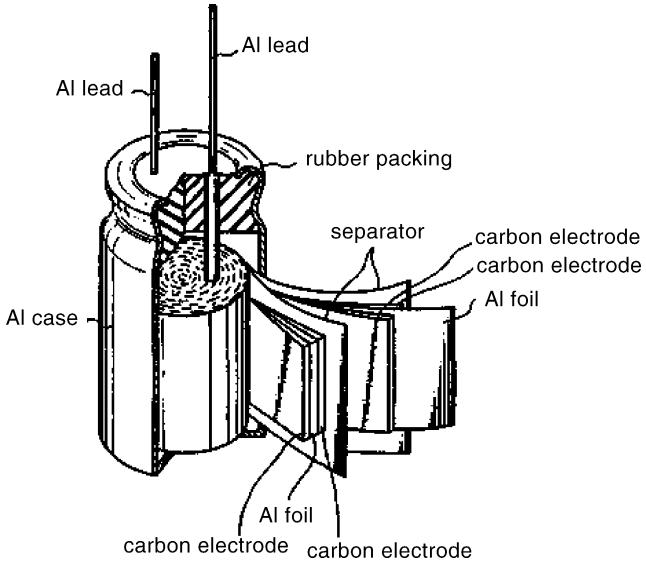

Fig. 1. A schematic view of Panasonic double layer capacitor.

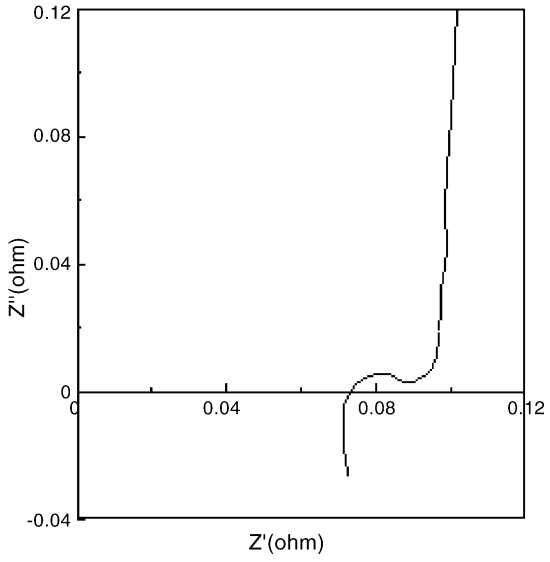

Fig. 2. The Nyquist plot measured from a Panasonic capacitor.

with a thickness of 50 μm when dry and 80 μm when wet was used as the separator. The wound body was then impregnated with an electrolyte. The electrode used in the capacitor was tetraethylammonium tetrafluoroborate salt (Et_4NBF_4) in propylene carbonate (PC) with a concentration less than 1 M. Therefore, the impregnated body was housed in an aluminum case with two aluminum lead wires and a rubber packing, as illustrated by Fig. 1. It is not difficult to see that the capacitor with spiral-wound structure consists two capacitors in parallel connected.

The capacitor was weight and measured. The AC impedance of the capacitor was measured. Then the wound body was removed from the aluminum can. The weight and dimensions of the components inside the capacitor such as electrode, current collector and separator paper were measured. Finally, the capacitor was then cut apart to examine the internal components.

3. Resistance measurement

AC impedance on the capacitor was preformed using a Solartron electrochemical unit (model 1280B) with frequency ranging from 10 to 20 kHz. During the AC impedance measurement, a sinusoidal source with an amplitude of 10 mV was supplied to the capacitor; all measurements were conducted at room temperature. Fig. 2 shows the Nyquist plot of the capacitor. An inductor behavior can be clearly seen at high frequencies due to the spiral-wound structure of the capacitor. From Fig. 2, it can be seen that the resistance of the capacitor was 0.078 Ω at 20 kHz, which corresponds to 15 $\Omega\,cm^2$ by assuming that the resistance is uniformly distributed in an electrode with the size of 24 cm × 2.4 cm and two cells are connected in parallel.

In order to understand the details of the resistance distribution inside the capacitor, resistances due to current collector, electrical lead to the current collector and separator paper were measured separately. The capacitor was opened, and the electrode and separator paper materials were removed from the capacitor for different resistance measurements. In the direction along the electrode surface, the resistance was mainly determined by the current collector. For the current collector, the resistance was measured using a standard four-probe method. For a 20 cm-long, 2.4 cm-wide and 20 μm-thick current collector, the resistance was 0.017 Ω. This value is significant compared to the total resistance of the capacitor. The resistivity of the current collector was calculated to be $4.08 \times 10^{-6}\,\Omega\,cm$, which is greater than the standard electrical resistivity of aluminum ($2.733 \times 10^{-6}\,\Omega\,cm$ at 300 K). The difference can be explained as follows. The standard value is the bulk aluminum resistivity, but the current collector used in EC capacitors is a 20 μm-thick aluminum foil. The surface roughness of the foil and the oxide layer at the surface increased the resistance of the Al foil. In addition, it was also found that the current collector used in EC capacitors is more brittle than the ordinary Al foil, but energy dispersive X-ray spectroscopic study showed that only Al was detected from the current collector. It is believed that the change of mechanical property was due to thermal or chemical treatments.

For the Al electrical lead, the total resistance of each electrical lead was less than 0.001 Ω. The Al electrical lead was welded to the current collector by an ultrasonic welder. Electrical leads were welded at the two electrode ends of 10 and 30 cm, respectively. The contact resistance between the electrical lead to the current collector was also measured using the four-probe method and was about 0.005 Ω. To compare with total resistance of the capacitor, both resistances contributed by the electrical lead and contact between electrical lead and current collector consider were negligible.

In the direction normal to the electrode surface, several resistances can be considered to be connected in series including electrical resistances from electrode and contact between electrode and current collector and ionic resistance from the separator paper. The separator paper was removed from the cell, and then sandwiched by two cylindrical stainless steel electrodes with polished surface and diameter of 1.27 cm. A mechanical force was applied to the stainless steel electrodes and was monitored by a force gauge. The ionic impedance was measured by an AC impedance meter in a frequency range of 1–20 kHz. Fig. 3 shows the resistance of the separator paper as a function of applied pressure at a frequency of 20 kHz. It can be seen that the resistance was insensitive to the applied pressure at pressures greater than 2 kg cm^{-2}, however, resistance increased at pressures less than 2 kg cm^{-2}. The increase in resistance at low applied pressure is simply due to the bad contact between the separator paper and electrodes. From Fig. 3, it was found that the resistance and resistivity of separator/electrolyte are about 11.5 Ω cm^2. In order to estimate the resistivity of the separator paper, the thickness of the separator paper was measured. It was found that the thickness of separator paper changed from ~50 μm when dry to ~80 μm when wet. The resistivity of the separator paper was calculated to be about 1400 Ω cm, which is more than 10 times greater than the resistivity of the electrolyte itself due to the porosity of the separator paper.

Two small pieces of electrode with the current collector were cut from the capacitor electrode and were laid face-to-face without separator paper in between. A pressure was applied to the electrode through two cylindrical stainless steel electrodes in order to study the pressure dependence. Four electrode probes were directly connected to the Al current collector in order to avoid the contribution of contact resistance between the Al current collector and stainless steel electrodes. Fig. 4 shows the measured resistance at different applied pressures. The resistance contributed by two different sources including electrical resistance of electrode materials (bulk and particles contact resistances) and electrical contact resistance between electrode and current collector. In order to distinguish these two resistances, Resistances for electrodes having different thickness were measured as follows. One carbon electrode was peeled off from the current collector; then the current collector was attached to another electrode for the resistance measurement. The thickness of the electrode was only half of that used previously. The resistance included value of one resistor from electrode and two resistors from contact between electrode and current collector. From these two measurements, the resistances due to the electrode and contact between electrode and current collector can be obtained as shown in Fig. 4, were 0.85 and 1.88 Ω cm^2, respectively, at an applied pressure of about 1 kg cm^{-2}. The thickness of the electrode was measured and was about 76 μm; the bulk resistivity of the electrode is about 112 Ω cm, which is quite high as a carbon electrode.

AC impedance of a single cell at different applied pressures was also measured. A small piece cell including current collectors, electrodes and separator paper was cut from the capacitor. Fig. 5 shows the resistance measured at 20 kHz

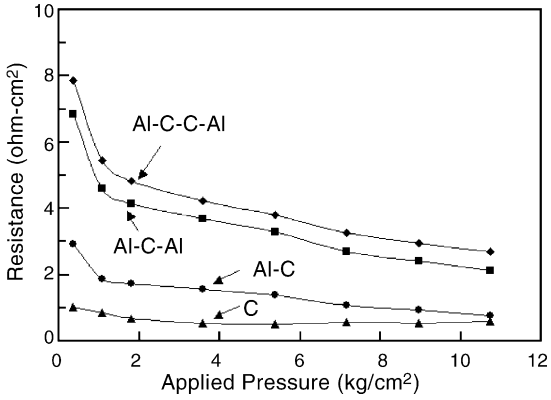

Fig. 4. The electrical resistance for two Al current collectors sandwiched two layers of electrode (Al–C–C–Al) and one layer of electrode (Al–C–Al) at different applied pressures. The data of (Al–C) and (C) is the results from the calculation and represents the contact resistance between the electrode and current collector and electrode, respectively.

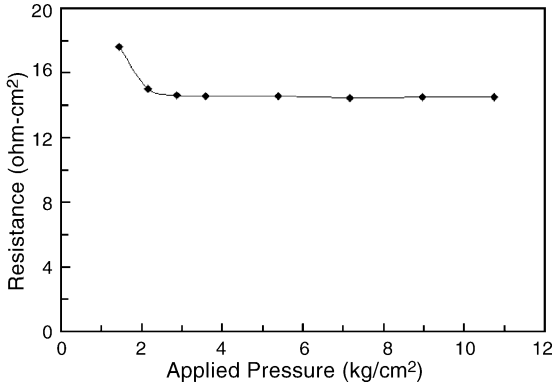

Fig. 3. The ionic resistance measured from the separator paper at different applied pressures. The separator paper was removed from Panasonic capacitor.

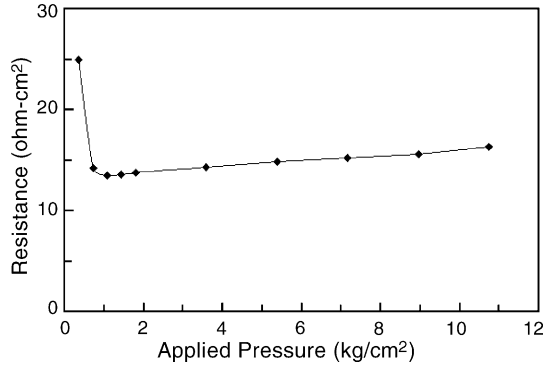

Fig. 5. The resistance of a single cell measured by AC impedance spectrometer at 20 kHz at different applied pressures.

at different applied pressures. It can be seen that at pressures less than 1 kg cm^{-2}, the resistance decreased with increasing the applied pressure; however, at pressures greater than 1 kg cm^{-2}, the resistance increased with increasing applied pressure. The minimum resistance of 13.5 Ω cm^2 was obtained at an applied pressure of about 1 kg cm^{-2}. The resistance value is about 10% less than that obtained from the estimation of total resistance of the capacitor. The difference is due to the current collector along the electrode direction. It will be discussed in the next section. It is not anticipated that the resistance will increased with increasing applied pressures, because for most electrochemical devices such as batteries and EC capacitors, the resistance of the device always decreases with increasing the pressure. From the above analysis, it can be seen that in the normal direction, the resistance mainly attributed to three sources including separator paper, electrode and contact between electrode and current collector. The resistance contribution by the electrode and contact must decrease with increasing applied pressure; therefore, the observation of the resistance increase as applied pressure increase must be attributed to the separator paper. It was ruled out that the resistance increase was due to the porosity of the separator paper decreased under applied pressure because of the following two reasons: (1) the ionic resistance of the separator was insensitive to the applied pressure as shown in Fig. 3. (2) It was found that the thickness of the separator paper did not change within the range of applied pressure. In order to understand such strange phenomenon, microstructures analysis of separator paper and electrode were studied by scanning electron microscope (SEM) and high-resolution optical microscope. Fig. 6(a) shows the SEM image of the separator paper. It can be seen that it is formed with fibers having size less than 20 μm in diameter. The fibers in order of micrometers perhaps are the binder in the separator paper. The porosity of the separator paper was estimated to be about 70% by measuring the weight difference of the separator paper wetted by water and when dry. It can also be seen that the separator paper formed with quite loose structure with some porous size greater than 100 μm, which might allow electrode material being squeezed into the separator paper under applied pressure. Fig. 6(b) shows the image of electrode surface from the optical microscope. The optical image provided a better depth profile than the SEM image because the electrolyte is transparent to visible light. It can be seen that the electrode was even more porous than the separator paper. A honeycomb shape and layer structure was observed. The weak connection between layer-to-layer is the possible reason for the high bulk resistivity of the electrode. From the above observation, it is believed that when the applied pressure was increased, the more carbon from the electrode was squeezed into voids in separator paper, which caused the effective porosity of the separator paper to be reduced as well as increased in ionic resistance of the separator paper. Because the layer structure of the electrode, the electrical connection from those carbons squeezed into separator paper to the main body of the electrode was not good. Therefore, the total resistance of the cell increased.

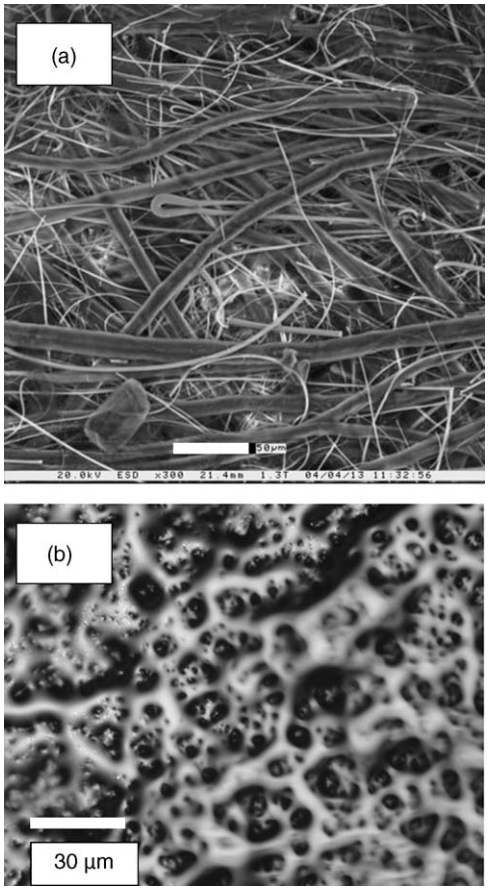

Fig. 6. (a) A SEM image of the surface of separator paper and (b) an optical microscopic photo of the surface of electrode.

Table 1 summarizes resistances measured from a single cell. It was found that the resistances contribution at normal direction were 10%, 22% and 68% from the electrode, contact between the electrode and current collector and separator paper, respectively. The sum of all resistances at normal direction was about 17 Ω cm^2, which was about 13% greater than the resistance measured by AC impedance spectrometer from a single cell. The inconsistency is believed due to the measurement error when the cell was cut and separated into different components.

Table 1
Measured resistances in a single cell

Sources	Resistance
Normal direction	
Electrode	1.7 Ω cm^2
Contact	3.76 Ω cm^2
Separator paper	11.5 Ω cm^2
Single cell	13.5 Ω cm^2
Along electrode direction	
Current collector	1.7 mΩ cm^{-1}

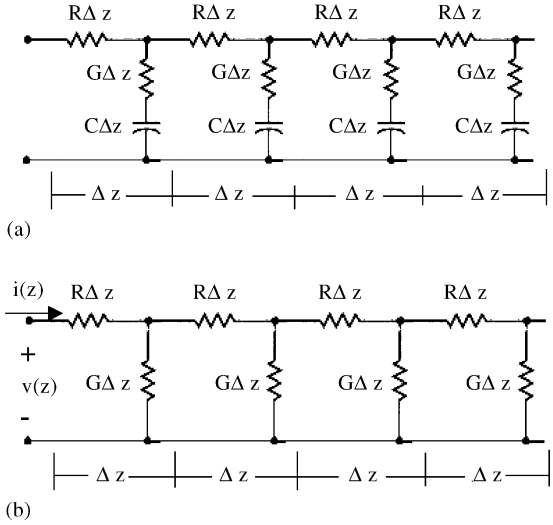

Fig. 7. A transmission line equivalent circuits (a) at low frequencies and (b) at high frequencies for describing capacitor with spiral-wound structure.

4. Transmission line model

The vector of current flowing in a capacitor with a spiral-wound structure can be projected in two directions, normal to and along with the electrode surface. The current flow and voltage drop along the electrode direction can be described by an equivalent circuit as shown in Fig. 7(a), which is widely used to represent electromagnetic wave transmission line. By considering two capacitors connected in parallel with an electrode width of 2.4 cm, in Fig. 7(a), R is the resistance of Al foil current collector and is 1.7 mΩ cm^{-1}; G the conductor of the capacitor at normal direction and is 0.355 S cm^{-1}; C is the capacitance and is 0.5 F cm^{-1}. It can be easily shown that at frequencies $f \gg G/2\pi C = 0.12$ Hz, such as at 20 kHz, the equivalent circuit can be simplified as shown in Fig. 7(b). The voltage and current in the circuit can be solved according to the following differential equations:

$$\frac{\partial v(z)}{\partial z} + Ri(z) = 0 \tag{1}$$

$$\frac{\partial i(z)}{\partial z} + Gv(z) = 0 \tag{2}$$

or

$$\frac{\partial^2 v(z)}{\partial z^2} - RGv(z) = 0 \tag{3}$$

$$\frac{\partial^2 i(z)}{\partial z^2} - RGi(z) = 0 \tag{4}$$

The general solutions for voltage and current are:

$$v(z) = V_o^+ e^{-\gamma z} + V_o^- e^{\gamma z} \tag{5}$$

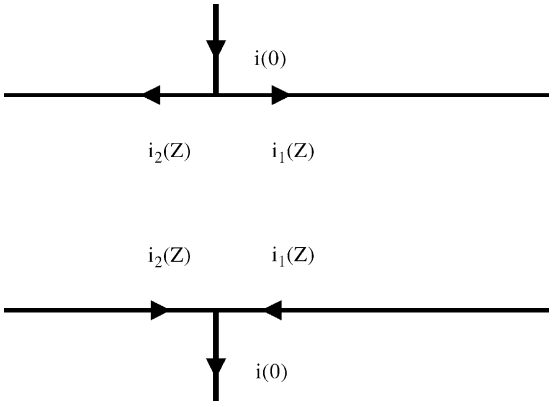

Fig. 8. A representation of current flow direction for a capacitor having electrical leads connected in the middle of electrode.

$$i(z) = I_o^+ e^{-\gamma z} + I_o^- e^{\gamma z} \tag{6}$$

where $\gamma = \sqrt{RG} = 0.0246\,\text{cm}^{-1}$ is called attenuation constant, the amplitudes (V_o^+, I_o^+) of the $+z$ propagating wave and (V_o^-, I_o^-) of the $-z$ propagating wave. To substitute $v(z)$ and $i(z)$ into Eqs. (1) and (2), it can obtained:

$$i(z) = \frac{V_o^+}{Z_o} e^{-\gamma z} - \frac{V_o^-}{Z_o} e^{\gamma z} \tag{7}$$

where $Z_o = \sqrt{\frac{R}{G}} = 0.069\,\Omega$, and is called the characteristic impedance. For a real capacitor, the electrode leads are welded in the middle of the electrode. It is assumed that the electrical lead located at $z = 0$, and right and left ends located at L_1 and L_2, respectively, as shown in Fig. 8, therefore, the length of electrode is $L = L_1 - L_2 = 40$ cm. There are two sets of solutions to describe the current flow to right and left part electrode and can be expressed as:

$$v_1(z) = V_1^+ e^{-\gamma z} + V_1^- e^{\gamma z} \quad \text{at } z \geq 0 \tag{8}$$

$$i_1(z) = \frac{V_1^+}{Z_o} e^{-\gamma z} - \frac{V_1^-}{Z_o} e^{\gamma z} \quad \text{at } z \geq 0 \tag{9}$$

and

$$v_2(z) = V_2^+ e^{-\gamma z} + V_2^- e^{\gamma z} \quad \text{at } z < 0 \tag{10}$$

$$i_2(z) = \frac{V_2^+}{Z_o} e^{-\gamma z} - \frac{V_2^-}{Z_o} e^{\gamma z} \quad \text{at } z < 0 \tag{11}$$

By using both open-end boundary conditions which are $V_1^+ = V_1^-$ and $V_2^+ = V_2^-$ at $z = L_1$ and $z = L_2$, respectively, and $V_1(0) = V_2(0)$. The voltage and current at $z = 0$ can be obtained as:

$$v(0) = V_1^+(1 + e^{-2\gamma L_1}) = V_2^+(1 + e^{2\gamma L_2}) \tag{12}$$

$$i(0) = \frac{V_1^+}{Z_o} \frac{(1 - e^{-2\gamma L_1})(1 + e^{2\gamma L_2}) + (1 + e^{-2\gamma L_1})(1 - e^{2\gamma L_2})}{1 + e^{2\gamma L_2}} \tag{13}$$

The resistance of the capacitor is:

$$Z(0) = \frac{v(0)}{i(0)} = Z_o \frac{(1 + e^{-2\gamma L_1})(1 + e^{2\gamma L_2})}{(1 - e^{-2\gamma L_1})(1 + e^{2\gamma L_2}) + (1 + e^{-2\gamma L_1})(1 - e^{2\gamma L_2})} \quad (14)$$

The voltage attenuation at both ends of electrode can also be obtained as:

$$\frac{v(L_1)}{V(0)} = \frac{2e^{-\gamma L_1}}{1 + e^{-2\gamma L_1}} \quad (15)$$

$$\frac{v(L_2)}{V(0)} = \frac{2e^{\gamma L_2}}{1 + e^{2\gamma L_2}} \quad (16)$$

Fig. 9(a) and (b) show the resistance of the capacitor and voltage attenuation at both ends of the electrode for electrical leads at different positions. From Fig. 9(a), it can be seen that when the electrical lead was welded at one of ends of the electrode, the resistance of the capacitor had the maximum value of 0.0914 Ω; when the welding position of the electrical lead was moved into the direction toward center of the electrode, the resistance of the capacitor decreased; and when the electrical lead was welded at the center of the electrode, the resistance of the capacitor reached to a minimum value of 0.0757 Ω. For a Panasonic capacitor, the electrical leads were welded at 10 cm from one end of the electrode. According to the transmission line model the resistance should be 0.0794 Ω, which is close to the value obtained from an AC impedance measurement. From Fig. 9(b), it can be seen that voltage attenuation along the electrode was also dependent on the position of the electrical lead. When the electrical lead was welded at one end of the electrode, the voltage at another end of the electrode was attenuated by about 34.4%; when the electrical lead was welded at the center of the electrode, the voltages at both ends were attenuated by about 11%. For the Panasonic capacitor studied in this project, the voltage attenuations were 22.2% and 3% at the two ends of electrode, respectively. Table 2 summarized voltage attenuation and resistance of the capacitor for electrical leads welded at different positions.

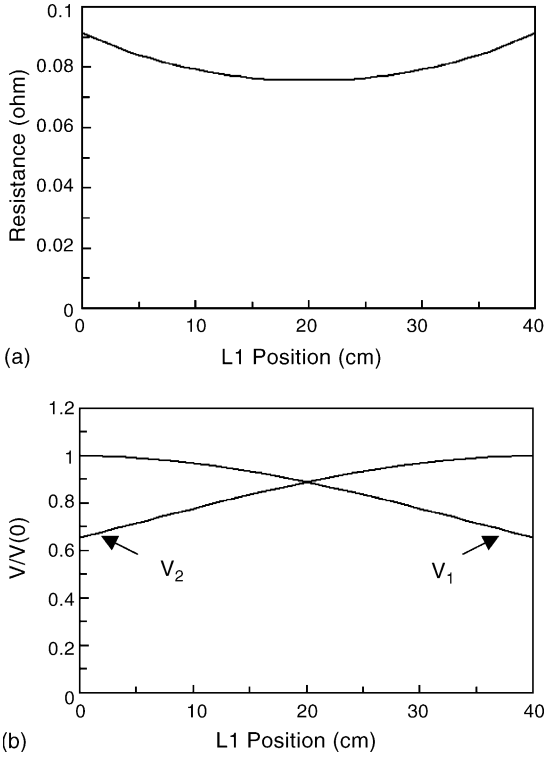

Fig. 9. (a) The resistance of the capacitor and (b) voltage attenuation at ends of electrode as a function of the position of electrical leads.

Table 2
Comparison of voltage attenuation and resistance for electrical leads wended at different positions

Lead position		Voltage attenuation		Resistance (Ω)
L_1 (cm)	L_2 (cm)	$V(L_1)/V(0)$	$V(L_2)/V(0)$	
40	0	0.656	1.00	0.0914
30	10	0.778	0.970	0.0794
20	20	0.890	0.890	0.0757

It should be pointed out that for capacitors using sputtering technique to sputter Al on the electrode ends, the resistance enhancements and voltage attenuations due to the position of electrical leads can be greatly diminished, because the current does not need to flow across the length of electrode, but only flow across the width of the electrode. Usually, the width of the electrode is much shorter than the length for the capacitor with spiral-wound structure. However, the Al sputtering on the electrode edges needed extra margin of current collector which may add additional volume and weight to the device, and also the cost of capacitor may be high; therefore, this technique is mainly used for the capacitors having large value of capacitance.

5. Conclusions

It has been demonstrated that the resistance distribution inside an EC capacitor with a spiral-wound structure can be analyzed. Resistances attributed to the electrical lead, electrode material, separator paper, contact between electrical lead and current collector and contact between electrode and current collector can be obtained by using DC four-probe method and AC impedance spectrometer. The resistance contributed by the current collector can be obtained by a combination of resistance measurements of the current collector and transmission line model analysis. For a Panasonic capacitor rated at 2.5 V and 10 F, it was found that the internal resistance is mainly attributed to 8.7% from the electrode, 19.2% from the contact between the electrode and the current col-

lector, 59.3% from the separator paper and 12.8% from the current collector.

Acknowledgements

This research was partially supported by the NASA-FAR Program under Grant No. NAG5-9420 and FSU Cornerstone Program.

References

[1] B. Conway, The Fourth International Seminar on Double Layer Capacitors and Similar Energy Storage Devices, Deerfield Beach, Florida, December 12–14, 1994.
[2] F.A. Posey, T. Morozumi, J. Electrochem. Soc. 113 (1966) 176–184.
[3] J.P. Zheng, Electrochem. Solid-State Lett. 2 (1999) 359.
[4] J.P. Zheng, J. Power Sources 137 (2004) 158.
[5] I. Tanahashi, A. Yoshida, A. Nishino, Bull. Chem. Soc. Jpn. 63 (1990) 2755.
[6] A. Yoshida, K. Imoto, US Patent No. 5,150,283 (1992).